

Inverse gas chromatography as a method for determination of surface properties of binding materials

Jihai Yu¹, Xiaolei Lu¹, Chunxia Yang², Baoli Du³, Shuxian Wang⁴, Zhengmao Ye^{1, 4*}

¹ Shandong Provincial Key Laboratory of Preparation and Measurement of Building Materials, University of Jinan, Jinan, Shandong Province, China

² School of Chemical and Chemical Engineering, University of Jinan, Jinan, Shandong Province, China

³ Dong Guan Chuang Jie New Materials CO., LED.

⁴ School of Material Science and Engineering, University of Jinan, Jinan, Shandong Province, China

*E-mail address: mse_yezm@ujn.edu.cn

Abstract. Inverse gas chromatography (IGC) is a promising measurement technique for investigating the surface properties of binding materials, which are the major influence element for the adsorption performance of superplasticizer. In this work, using the IGC method, blast furnace slag (BFS), sulphotoaluminate cement (SAC) and portland cement (P·O) are employed to systematically evaluate the corresponding dispersive component (γ_s^d), specific surface free energy (γ_s^{ab}), and acid-base properties. The obtained results show that γ_s^d contributes to a major section of the surface free energy in the three binding materials, suggesting they are of a relatively low polarity. Compared to the two kinds of cements, the BFS possesses the highest dispersive and specific surface free energies (the values are 45.01 mJ/m² and 11.68 mJ/m², respectively), and also exhibits a wider distribution range of γ_s^d , indicating their surfaces are heterogeneous. For acid-base properties, the results indicate the surfaces of three samples are basic in nature. In addition, the adsorption investigation shows that per unit surface of BFS adsorbs the most superplasticizer molecules, which indicates the higher surface free energies is beneficial to the superplasticizer adsorption.

1. Introduction

The Binding materials cooperated by superplasticizer are widely used in building industry. The adsorption capability of binding materials surfaces would influence the water reducing effect of the superplasticizer. QU *et al.*, reported that the adsorption of cement particles was influenced by many factors such as mineral composition of cement, alkali sulphate and mineral admixture in cement ^[1]. S.K. Agarwal *et al.*, found that different grade of P·O showed different compatibility with superplasticizer ^[2]. Erdogdu. S. showed that the mineral composition of cement will influenced the adsorbed capability of cement particles and the effect of a superplasticizing admixture depended on the composition of cement rather than the amount used ^[3]. Surface free energy is also an important influential element for the performance of binding materials, there are few reports about the relationship between the adsorption capability and surface free energy nevertheless. Although the traditional thin-layer wicking technique has been employed by some researchers to study the dynamic



contact angles and surface free energy of cement binding materials^[4], the experimental conditions are usually difficult to be controlled.

As an alternative to classic contact angle measurement, IGC has proved to be a sensitive and easy-operating technique for the characterization of materials surface properties of^[5-7], and are widely applied in the fields of food detection and composite materials. Surface energy analysis technique based on IGC has been found to be very effective for characterizing wetting phenomena on powders and fibers^[8-10]. Lubomír Lapčík used the IGC for the measurement of the surface energy of demineralised whey and skimmed milk and showed the surface energy profiles^[11]. Jeong et al., studied the surface properties of CaCO₃ by IGC^[12]. Naveed Arsalan et al., introduced the IGC to characterize the surface energy of sandstones (Ottawa sand and Berea sandstone)^[13], and they indicated that the use of IGC enables an accurate picture of the surface at different temperatures and other physical conditions by taking into account surface heterogeneity and the interaction forces responsible for the adsorption^[14]. Therefore, based on the studies as mentioned above, the IGC method may be also suitable for analyzing the surface properties of binding materials.

In this study, we investigate the surface properties by the IGC method. The adsorption weight of naphthalene based superplasticizer on the surface of binding materials is also measured. Combining the surface energy test and adsorption capacity measurement, there is a positive relevance between surface energy and adsorption capacity of binding materials particles. The relevance between surface properties and superplasticizer adsorption on binding material surfaces should be further studied by the IGC method.

2. Materials and methods

2.1. Materials

Some SAC, P·O and BFS were produced by factories in Shandong Province. The chemical components and physical properties of the materials are listed in Table 1.

Table 1 Chemical composition and physical properties of cement (wt %).

Material	SiO ₂	Fe ₂ O ₃	Al ₂ O ₃	CaO	MgO	SO ₃	Specific Surface Area (m ² ·g ⁻¹)
SAC	10.96	3.71	28.9	45.25	1.45	8.88	2.2
P·O	19.95	2.90	4.71	60.58	1.41	—	2.0
BFS	32.31	0.29	16.36	35.53	10.41	2.74	1.26

* Specific surface area of binding materials is measured by a commercial inverse gas chromatograph SMS IGC-SEA (surface measurement systems, UK).

Values of Gutmann's donor and modified acceptor numbers for the polar probes are displayed in Table 2

Table 2 Physical constants of the probes used in the IGC measurements^[15-17].

Probes	$a(\times 10^{-19} \text{ m}^2)$	γ_1^d (mJ/m ²)	$a(\gamma_1^d)^{0.5}$ [m ² (mJ)/ m ²) ^{0.5}]	Modified acceptor numbers(kJ/mol)	Gutmann's donor (kJ/mol)	Specific characteristic
n-Heptane	5.73	20.3	2.58×10^{-18}	-	-	Neutral
n-Octane	6.28	21.3	2.89×10^{-18}	-	-	Neutral
n-Nonane	6.89	22.7	3.28×10^{-18}	-	-	Neutral

n-Hexane	5.10	18.4	2.19×10^{-18}	-	-	Neutral
Ethyl acetate	3.30	19.6	1.46×10^{-18}	6.3	71.8	Amphoteric
Dichloromethane	2.45	24.5	3.83×10^{-18}	16.4	0.0	Acid
Acetonitrile	2.14	27.5	1.12×10^{-18}	19.4	58.3	Amphoteric

2.2. Methods

2.2.1 IGC method. The IGC test was carried out using a commercial inverse as chromatograph SMS IGC-SEA (surface measurement systems, UK). The injection system used by the SMS IGC-SEA allows the precise control of the injection size, and therefore different amounts of probe vapor can be chosen to pass through the sample column achieving different surfaces coverage (n/nm). If a series of probe vapors is injected at the same surface coverage, the surface free energy and Gibbs specific free energy values can be determined. Consequently, the injections of probe vapors at different surface coverage will be referred to as a surface free energy profile. The surface chemistry of the samples was assessed using the Gutmann acid (Ka) and base (Kb) numbers, determined based on the Gutmann approach using the following polar probes: Dichloromethane, Ethyl acetate, Acetonitrile, Chloroform.

Ka and Kb values of the samples were calculated using the γ_s^{ab} values of polar probes at that particular surface coverage.

In IGC, the term “inverse” indicates that the solid state materials to be characterized was packed into the chromatographic column and this material was probed by known gas mixtures which were injected into the column [18]. For the preparation of columns, 250mg of the powder was filled into a salinized standard column (3mm ID, 300mm long) using the SMS sample-packing device. All the columns have been prepared using the same batch of material and using the same frequency and duration of tapping during packing.

The stationary phase characterization was achieved by portioning the sample between the mobile phase and the stationary phase, indicated by the time taken to elute the samples. The molecular probes were injected at infinite dilution in order to rule out lateral probe-probe interactions and favor probe-stationary phase interactions only [19]. The dead volume was determined by injecting methane, a probe molecule that does not interact significantly with low energy materials.

The total surface free energy of solid materials is often divided into dispersive γ_s^d and specific (γ_s^{ab}) parts, as is shown in Equation 1. Dispersive (apolar) interactions, also known as Lifshitz-van der Waals interactions, consist of London, Keesom and Debye interactions. Specific (polar) interactions explain all other types of interactions [20].

$$\gamma_s = \gamma_s^d + \gamma_s^{ab} \quad (1)$$

A standard IGC method for determining γ_s^d of the stationary phase relies on a series of linear alkane molecular probes. The increasing carbon numbers in the chain lead to the increase of adsorption energy. The n-alkane line is obtained by plotting the adsorption free energy of probes against the carbon number n of the injected alkane probes. In this method, a plot of $RT \ln(V_{N,n})$ versus the carbon number (of alkanes) should produce a linear correlation. Where R is the gas constant $8.31 \text{ J mol}^{-1} \text{ K}^{-1}$, T is the temperature; $V_{N,n}$ is the retention volumes of the n-alkanes probes with carbon number n . The dispersive component of the solid sample can be determined from the slope of the correlation.

$$-\Delta G_{CH_2} = 2(\gamma_{CH_2} \gamma_s^d)^{1/2} N_A a_{CH_2} \quad (2)$$

Where γ_s^d is the dispersive component of the solid surface free energy, a_{CH_2} is the cross sectional area of the methylene group, γ_{CH_2} is the surface dispersive free energy of a solid material constituted solely of methylene groups. N_A is Avogadro's number, ΔG_{CH_2} is the slope corresponds to the increment of free energy per methylene groups [21].

Specific surface free energy can be examined from the probes plot of $RT \ln V_N$ against $a(\gamma_i^d)^{0.5}$. The distance between the ordinate values of the polar probe datum point and the n-alkane reference line gives the specific component of the surface free energy.

$$\frac{\gamma_s^{ab}}{AN^*} = \frac{DN}{AN^*} K_a + K_b \quad (3)$$

DN and AN^* are Gutmann's donor and modified acceptor numbers, respectively. K_a and K_b are obtained from a plot of $-\frac{\gamma_s^{ab}}{AN^*}$ versus $\frac{DN}{AN^*}$ with K_a as the slope and K_b as the intercept.

The overall acid-base character of the samples' surface can be evaluated from the K_b/K_a ratio^[22].

2.2.2 Adsorption test. Naphthalene based superplasticizer (NBS) was used as adsorbent. Before this test, NBS solutions with different concentration were taken for ultraviolet spectrophotometry to find the characteristic absorption peak, as is shown in the Figure 1. A curve of concentration to absorbance can be obtained by linear fitting method at the wavelength of 229 nm, which was shown in Figure 2. In the test, 2 g of cement were put into 200 g NBS agent solution with the concentration of 6mg/L to get the suspension of cement particles. A certain amount of suspension was taken out for centrifuging and the supernatant was taken for ultraviolet spectrophotometry. Then the absorbance of the supernatant can be got. The weight of NBS adsorbed by cement particles could be calculated referring to the standard adsorption curve of the NBS.

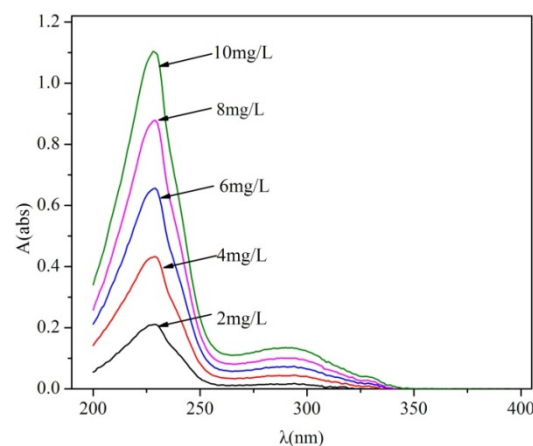


Figure 1 Adsorption spectra of NBS standard solution.

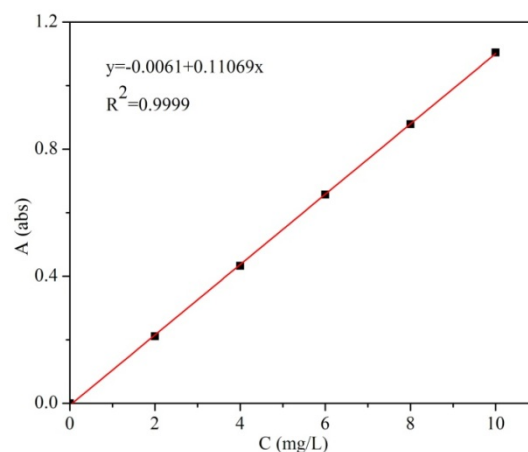


Figure 2 Standard adsorption curve of NBS.

3. Results and discussion

3.1 Dispersive surface free energy profiles and distribution

The dispersive surface free energy profiles (γ_s^d) of cement and BFS are displayed in Figure 3. The calculate γ_s^d of SAC, P·O and BFS fell into the ranges of 41.35-51.99 mJ/m², 40.5-53.01 mJ/m² and 41.89-58.56 mJ/m², respectively. The finally adoptive γ_s^d of the three materials are 43.34, 42.55 and 45.01 mJ/m² respectively.

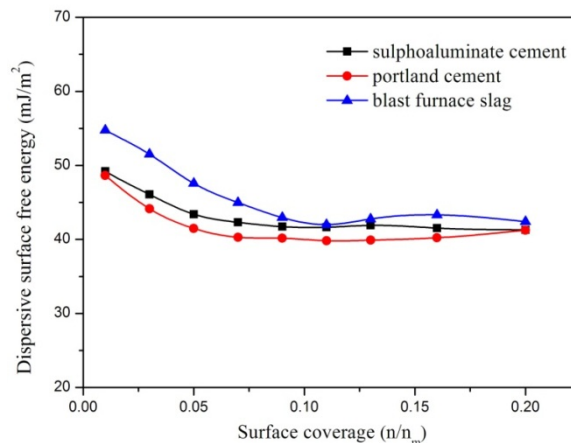


Figure 3 Dispersive surface free energy profiles of binding materials

As is shown in Figure 3, it can be seen that the γ_s^d values for SAC, P·O and BFS showed a decreasing trend with an increase in the surface coverage. The γ_s^d showed the highest value when the coverage is 0.01%. The retention volume of samples decreased with increasing surface coverage, because the interaction between the alkane probes and less energetic sites at high surface coverage was weaker [23-25]. The γ_s^d values for samples decreased remarkably as the surface coverage increased from 0.01% to 0.13% then increased slightly with still greater surface coverage. This may be because the samples surfaces are heterogeneous and rough [20].

The Figure 4 displayed the distribution of dispersive surface free energy of three samples. It showed a characteristically broader distribution for BFS (42.39 mJ/m² to 54.78 mJ/m²). The dispersive surface free energy distribution of SAC and P·O were narrower, ranging from 41.30 mJ/m² to 49.20 mJ/m² and 41.27 mJ/m² to 48.63 mJ/m² respectively with relatively the same area increment occupancy of 2%.

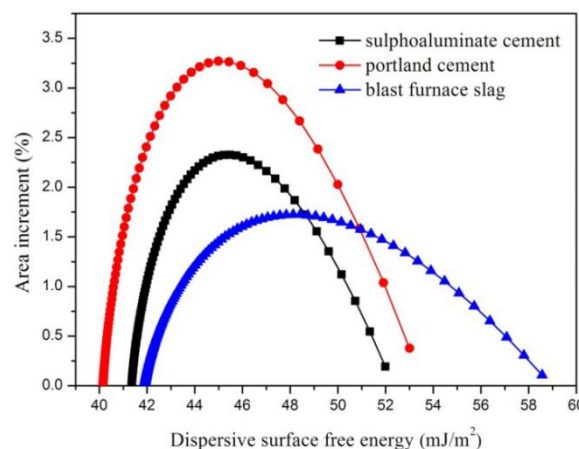


Figure 4 Dispersive surface free energy distributions of binding materials

Surface energy values are inherently independent of surface area, particle size, and particle shape. For some materials (such as silica and fiber) high surface area is associated with high surface free energy [17, 26]. However, in some cases it is not true, because a larger surface area implies a higher

concentration of active sites or even a change in composition per unit surface. In theory, the surface free energy values will not be affected by changes in surface roughness. However, the orientation and interaction of IGC probe molecule can vary slightly if surface roughness is of the same magnitude as the molecular probe diameters ^[21]. Thus the surface free energy is not only associated with structural variations, but also with the density or type of functional groups orientated on the surface. In this study, the three samples have different composite and surface rough, so the dispersive surface free energy was affected by various factors.

3.2 Specific surface free energy and acid-base surface characteristics

Specific surface free energy can be examined from the probes plot of $RT \ln V_N$ against $a(\gamma_l^d)^{0.5}$. The distance between the ordinate values of the polar probe datum point and the n-alkane reference line gives the specific component of the surface free energy. The results show that the specific surface free energy (γ_s^{ab}) of the three binding materials are 7.43, 8.20 and 11.68 mJ/m² respectively.

Acid-base surface characteristics of samples depend on the ability to participate in specific interactions. The K_a and K_b were used for characterization of the acidity or basicity of the surface of samples. The surface chemistry of samples is routinely characterized by Gutmann's acid-base theory. If $K_b/K_a > 1$, the surface can be considered to be basic, meaning the surface of the solid prefers to donate electrons, while $K_b/K_a < 1$, the surface can be considered to be acidic, indicating that it prefers to accept electrons. The K_b/K_a ratios were 5.20, 4.49 and 3.01 for SAC, P·O and BFS respectively. This indicated that the surface of samples is basic in nature. The basic character of SAC is stronger than the others.

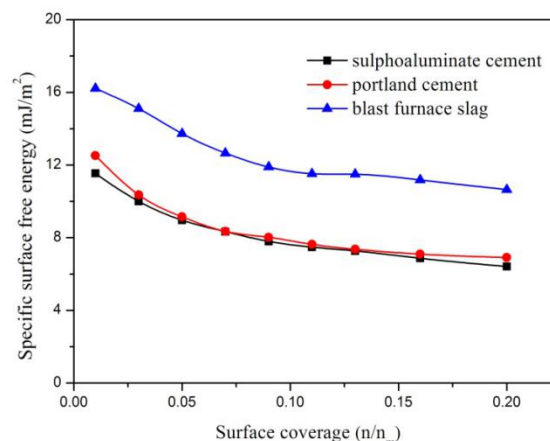


Figure 5 Specific surface free energy profiles of binding materials

As is shown in the Figure 5 the specific surface free energy of BFS was still the highest which is the same case for dispersive surface free energy. It is similar for the specific surface free energy of SAC and P·O.

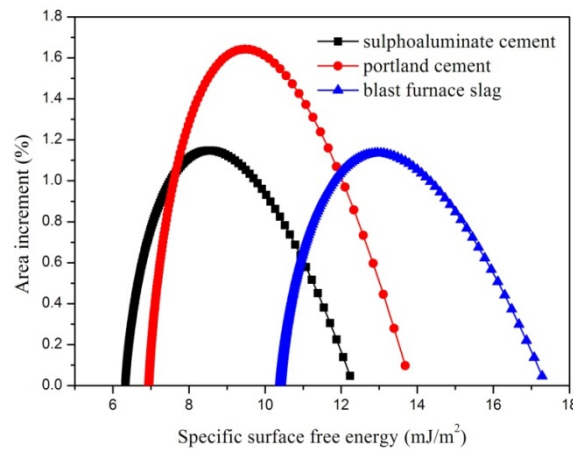


Figure 6 Specific surface free energies distributions of binding materials

Figure 6 displayed the specific surface free energy distribution, it can be found from the picture that the specific surface free energy distribution range of three samples were similar. This was different from the dispersive surface free energy distribution. It shows that the dispersive surface free energy and specific surface free energy were influenced by different factors.

3.3 Adsorption properties

The experiment results of ultraviolet spectrophotometry listed in Table 3 showed that the adsorption capacity of BFS was the highest. The mass of NSP in the suspension can be calculated by the standard absorption spectrum of naphthalene based SP then the absorbance of NSP by binding materials can be calculated. The weight of NSP adsorbed by unit surface of SAC, P·O and BFS were 0.161mg, 0.155mg and 0.175mg respectively. The result was corresponding to the laboratory finding of LIU et al., [27]. They found that the adsorbing capacity of SAC is higher than the adsorbing capacity of P·O.

To counteract the effect of specific surface area on the weight of NSP adsorbed. The weight of superlasticizer adsorbed by unit surface of samples was measured. The weight of NSP adsorbed on unit surface of three samples is 0.161 mg, 0.155mg, and 0.175mg respectively. The NSP adsorption capacity of BFS is the strongest.

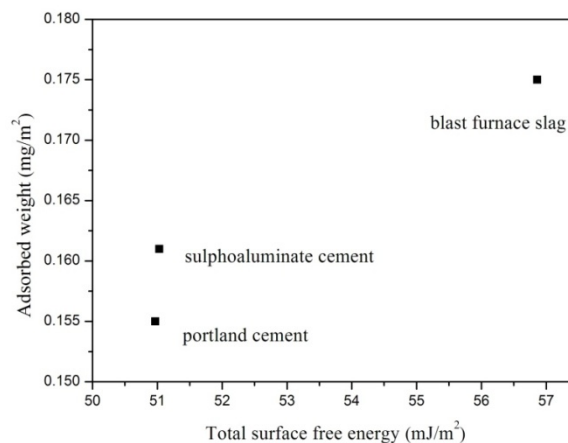


Figure 7 Adsorption weight by unit surface versus total surface free energy

As is shown in Figure 7 there is a positive correlation between surface free energy and adsorption capacity of samples. However the influencing mechanism of surface free energy on adsorption capacity of binding material is complicated and many works are needed to be done to establish the accurate relationship between surface free energy and adsorption. The IGC method will be an important technology in the study.

4. Conclusion

The γ_s^d value significantly decreased with the increasing of surface coverage from 0.01% to 0.13% then slightly increased during the increasing of surface coverage from 0.13% to 0.2%. This maybe because that the samples are heterogeneous and rough. The γ_s^d values of SAC, P·O and BFS fell into 41.5-49.3 mJ/m², 41.2-48.7 mJ/m² and 42.4-54.8 mJ/m² respectively. The BFS particles exhibits relatively wider range of γ_s^d distribution so its surface is more heterogeneous. Both the three binding materials are basic in nature. BFS showed higher values in both dispersive surface free energy and specific surface free energy. The unit surface of BFS adsorbed the most NSP molecules. Combining the measurement results of surface free energy and adsorption capacity of the samples it showed that the adsorption capacity of sample particles increases with higher surface free energy. IGC method is alternative for investigation of binding materials, and has potential advantages for the study of binding materials surface. The application of IGC in binding materials industry should be further explored.

Acknowledgements

This work is supported by National Natural Science Foundation of China (No. 51272092 No. 51302105) and Shandong Provincial Science and Technology Major Project (New Industry) (No. 2015ZDXX0702B01). Meanwhile, this work is supported by Program for Scientific Research Innovation Team in Colleges and Universities of Shandong Province.

References

- [1] Qu JD, Peng JH, Chen MF, Zhang JX, Wan TZ, (2005) The research progress of adsorption properties of water reducers on the cement particles Journal of Building Materials 8: 410-417.
- [2] Agarwal SK, Masood I, Malhotra SK, (2000) Compatibility of superplasticizers with different cements Construction and Building Materials 14: 253 -257.
- [3] Erdogdu S, (2000) Compatibility of superplasticizers with cements different in composition Cement and Concrete Research 30: 767 -773.
- [4] Liu JP, Li H, Tian Q, Wang YJ, (2013) Determination of dynamic contact angles of cement and mineral admixtures based on thin-layer wicking technique Journal Of Southeast University(Natural Science Edition) 43: 1074-1079.
- [5] Gamelas JAF, Ferraz E, Rocha F, (2014) An insight into the surface properties of calcined kaolinitic clays: the grinding effect Colloid. Surface A 455: 49–57.
- [6] Ylä-Mäihäniemi PP, Heng JYY, Thielmann F, Williams DR, (2008) Inverse gas chromatographic method for measuring the dispersive surface energy distribution for particulates, Langmuir 24: 9551–9557.
- [7] Riedl B, Matuana LM, (2006) Inverse gas chromatography of fibers and polymers, Encyclopedia of Surface and Colloid Science, 3018–3031.
- [8] Lapčík L, Kubiček P, Lapčíková B, Zbořil R, Nevěčná T, (2014) Study of penetration kinetics of sodium hydroxide aqueous solution into wood samples. BioResources 9: 881–893.
- [9] Martinez-Padilla LP, Garcia-Mena V, Casas-Alencaster NB, Sosa-Herrera MG, (2014) Foaming properties of skim milk powder fortified with milk proteins. International Dairy Journal 36: 21–28.
- [10] Lazar P, Otyepková E, Banáš P, Fargašová A, Šafářová K, Lapčík L, (2014) The nature of high surface energy sites in graphene and graphite. Carbon 73: 448–453.
- [11] Lapčík JR, Lapčík L, De Smedt S, Demeester J, Chabreček P, (1998) Hyaluronan: Preparation, structure, properties and applications. Chemical Reviews 8: 2663–2684.
- [12] Jeong SB, Yang YC, Chae YB, Kim BG, (2009) Characteristics of the treated ground calcium carbonate powder with stearic acid using the dry process coating system, Mater. Trans. 50: 409–414.
- [13] Arsalan N, Palayangoda SS, Burnett DJ, Buiting JJ, Nguyen QP, (2013) Surface energy characterization of sandstone rocks, Journal of Physics and Chemistry of Solids, 74: 1069-1077.
- [14] Arsalan N, Palayangoda SS, Burnett DJ, Buiting JJ, Nguyen QP, (2013) Surface energy

- characterization of carbonate rocks, *Colloids and Surfaces A: Physicochemical and Engineering Aspects*, 436: 139-147.
- [15] Karaoglan GK, Sakar D, (2011) Surface characterization of a novel D-p-D type ligand by IGC at infinite dilution *Chromatographia* 73: 93–98.
- [16] Steele DF, Moreton RC, Staniforth JN, Young PM, Tobyn MJ, Edge S, (2008) Surface energy of microcrystalline cellulose determined by capillary intrusion and inverse gas chromatography *AAPS J.* 10: 494–503.
- [17] Cordeiro N, Gouveia C, Moraes AGO, Amico SC, (2011) Natural fibers characterization by inverse gas chromatography. *Carbohydr. Polym* 84: 110–117.
- [18] Perruchot C, Chehimi MM, Vaulay MJ, Benzarti K, (2006) Characterisation of the surface thermodynamic properties of cement components by inverse gas chromatography at infinite dilution. *Cem. Concr. Res.* 36: 305–319.
- [19] Voelkel A, (2004) Inverse gas chromatography in characterization of surface. *Chemometr. Intell. Lab.* 72: 205–207.
- [20] Yao ZT, Ge LQ, Ji XS, Tang JH, Xia MS, Xi YQ, (2015) Surface properties studies of bivalve shell waste by the IGC technique: Probing its significant potential application in the polymer industry. *Journal of Alloys and Compounds* 621: 389-395.
- [21] Thielmann F, Butler D, Determination of the dispersive surface energy of Paracetamol by iGC at infinite dilution, *SMS Application Note* 202
- [22] Gutmann V, *The Donor–Acceptor Approach to Molecular Interaction* Plenum Press, 1978.
- [23] Ho R, Hinder SJ, Watts JF, Dilworth SE, Williams DR, Heng JYY, (2010) Determination of surface heterogeneity of d-mannitol by sessile drop contact angle and finite concentration inverse gas chromatography. *Int. J. Pharmaceut* 387: 79–86.
- [24] Burnett DJ, Khoo J, Naderi M, Heng JYY, Wang GD, Thielmann F, (2012) Effect of processing route on the surface properties of amorphous indomethacin measured by inverse gas chromatography. *AAPS PharmSciTech.* 13: 1511–1517.
- [25] Lapčík L, Otyepková E, Lapčíková B, Otyepka M, (2013) Surface energy analysis (SEA) study of hyaluronan powders. *Colloid. Surface A* 436: 1170–1174.
- [26] Zhang WJ, Leonov AI, (2001) IGC study of filler–filler and filler–rubber interactions in silica-filled compounds. *J. Appl. Polym. Sci.* 81: 2517–2530.
- [27] LIU T, LI YJ, CHEN J, YANG W, WU X, (2013) The research of adsorption of naphthalene-based superplasticizer on alite-sulphoaluminate cement. *Concrete* 20: 73-76.